AEROSPACE INFORMATION REPORT

AIR1904™	REV. B

Issued 1985-12
Revised 2001-12
Reaffirmed 2022-09

Superseding AIR1904A

Tire Spray Suppression - Airplane Design and Consideration for

RATIONALE

AIR1904B has been reaffirmed to comply with the SAE Five-Year Review policy.

1. SCOPE:

This SAE Aerospace Information Report (AIR) relates considerations for design test procedures and test data evaluation for qualification of tire spray deflection devices.

1.1 Purpose:

The purpose of tire spray deflection devices is to prevent ingestion of water or slush into engines, or to limit ingestion to non-hazardous quantities. A further purpose may be to prevent impacting of the deflected spray into pusher propellers or upon other parts of the aircraft in a harmful manner. These deflection devices may be an integral part of the tire, or may be installed on the landing gear or upon other parts of the aircraft. Considerations should cover all applicable ground operating modes including use of reverse thrust, and be extended to cover possible damage to mechanisms, systems, antennae, or pitot and static ports.

Ingestion of tire deflected water or slush has caused powerplants to lose power when no precautions were taken. Certification requires establishment of safe and acceptable air vehicle operation under flooded and slush covered runway conditions. Past aircraft operations have shown that there is a need to substantiate the capability of aircraft to operate safely from runways having standing water or slush over all or parts of the surface.

TO PLACE A DOCUMENT ORDER: **Tel: 877-606-7323 (inside USA and Canada)**
Tel: +1 724-776-4970 (outside USA)
Fax: 724-776-0790
Email: CustomerService@sae.org
SAE WEB ADDRESS: **http://www.sae.org**

For more information on this standard, visit
https://www.sae.org/standards/content/AIR1904B/

2. REFERENCES:

FAA Advisory Circular No. AC 91-6A Water, Slush, and Snow on the Runway, dated May 24, 1978.

FAA Advisory Circular No. AC 20-124 Water Ingestion Testing for Turbine Powered Airplanes, September 30, 1985.

FAA Advisory Circular No. AC33-2B Aircraft Engine Type Certification Handbook, June 30, 1993.

NASA Technical Note D-552, Studies of the Retardation Force Developed on an Aircraft Tire Rolling in Slush or Water, September 1960.

NASA Technical Paper 2718 Measurements of Flow Rate and Trajectory of Aircraft Tire-Generated Water Spray, July 1987.

FAA Regulation FAR 23.1091 (c) (2) Air Induction System, January 1, 1998.

FAA Regulation FAR 25.1091 (c) (2) and (d) (2) Turbine Engine Air Induction Location.

FAA Regulation FAR 25.1323 (d) Airspeed Indicating System - Port Locations.

Joint Airworthiness Regulations JAR 25.1091 Air Intake.

Advisory - Joint ACJ 25.1091 (d) (2) &(e).

Validation Note No. 3, Special Condition 9 Take off from Precipitation Covered Runways.

SAE Technical Paper 861626, Flow Rate and Trajectory of Water Spray Produced by an Aircraft Tire.

Royal Aircraft Establishment of England Report, The Measurement of the Effects of Slush and Water on Aircraft During Takeoff.

3. HISTORICAL REFERENCE:

Engineers recognized, during the early days of jet-powered operations, that there were safety implications for jet engines subject to foreign object ingestion from materials thrown from the wheels and tires of these aircraft. Various studies and engineering approaches to solving the problems associated with the ingestion of water spray from operations on flooded runways began evolving in those early years. Chine tires were one of the most common devices developed to help prevent landing gear propelled water from entering engines.

Some aircraft have fortunate aerodynamic geometries such that wheel and tire deflected water and slush plumes stay clear of engines and other sensitive areas. Aerodynamic designs to purposefully accomplish this end are the ideal.

3. (Continued):

In several instances, the process of “stretching" an airframe has introduced an ingestion problem that had not existed in original models. Figure 1 illustrates this possibility.

Recent developments in rear mounted propeller driven aircraft have opened a new set of parameters to be considered in water deflection. Portions of the following document may well apply to such aircraft, but at present publication no specific efforts have been so directed. Hopefully, future revisions or supplementary efforts will cover those concerns.

4. DESIGN CONSIDERATIONS FOR SPRAY SUPPRESSION:

4.1 Deflection of Spray Necessitated By:

a. Engine performance (surges, loss of thrust, inlet blockage)

A loss of sustained engine power or thrust under the influence of ingestion of water, ice, or hail has been recognized by the Federal Aviation Administration (FAA) as a safety issue in Advisory Circular No. AC 33-2B. Paragraph 53 (c) of this Advisory Circular stipulates that ingestion of water, ice, or hail may not cause sustained power loss or thrust loss or require engine shut down. The paragraph also says that the ability of the engine to safely accelerate and decelerate while inducting a mixture of at least 4 percent water by weight of engine airflow must be demonstrated at both flight idle and takeoff power settings.

b. Static port performance (icing, blockage)

c. Mechanisms (impact damage, clogging, freezing)

d. Landing performance (effect on thrust reverser performance)

e. Takeoff performance (slush drag)

A loss of takeoff performance when operating from slush-covered runways has been recognized as evidenced by Federal Aviation Administration (FAA) Advisory Circular No. AC 91-6. Jet transports with high takeoff speeds and low acceleration characteristics can be exposed to drag forces that may inhibit takeoff. The term “slush drag” is used to encompass either slush or water drag. Research into the problem showed that slush, or any other fluid which can remain on a runway in sufficient depth, causes drag on the aircraft in two ways. First, there is a direct drag on the wheels as they displace fluid from their path, while second, the intense spray formed by this process causes drag by impingement on the aircraft structure. National Aeronautics and Space Administration (NASA) research and experience show that the total impingement drag can be great enough for certain airplane types to cause marginal takeoff capability in 1 inch of slush and to cause takeoff refusal in 1.5 to 2 inches of slush depth. See Figure 2.

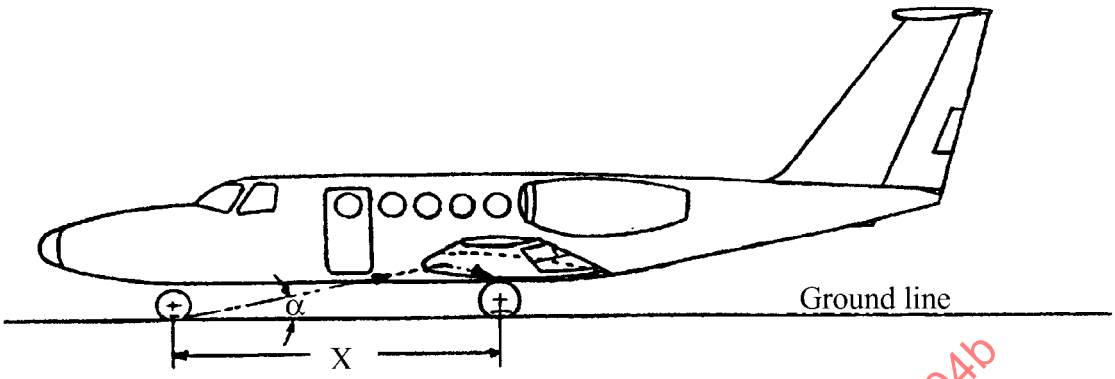

Original model

X = wheelbase
X + Y = stretched wheelbase generated by adding a fuselage plug between the main and nose gear
α = angle of spray pattern generated by nose wheel

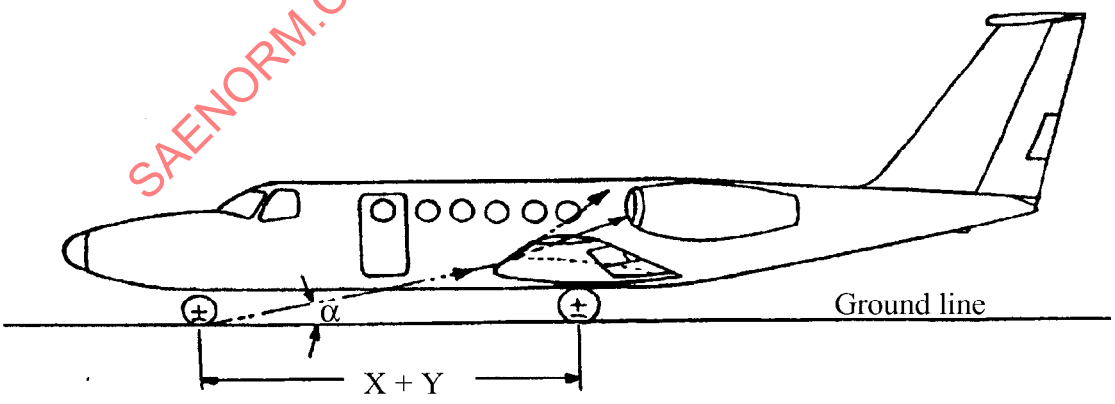

Stretched model

FIGURE 1 - Typical Aircraft Model Configurations

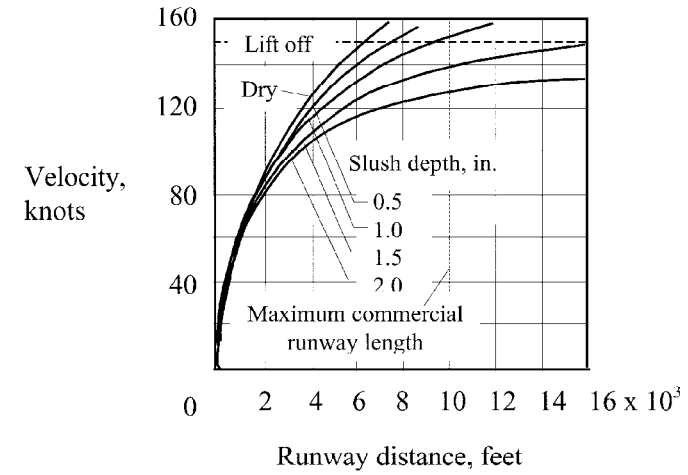

Four-Engine Jet Transport	
Gross weight	210 000 lbf
Altitude	sea level
Temperature	42°F
Wind	7.3 knots head wind
Runway slope	zero
Flaps	30 degrees
Engines	(4) operating at Dry takeoff thrust
Takeoff thrust	13 000 lbf/engine

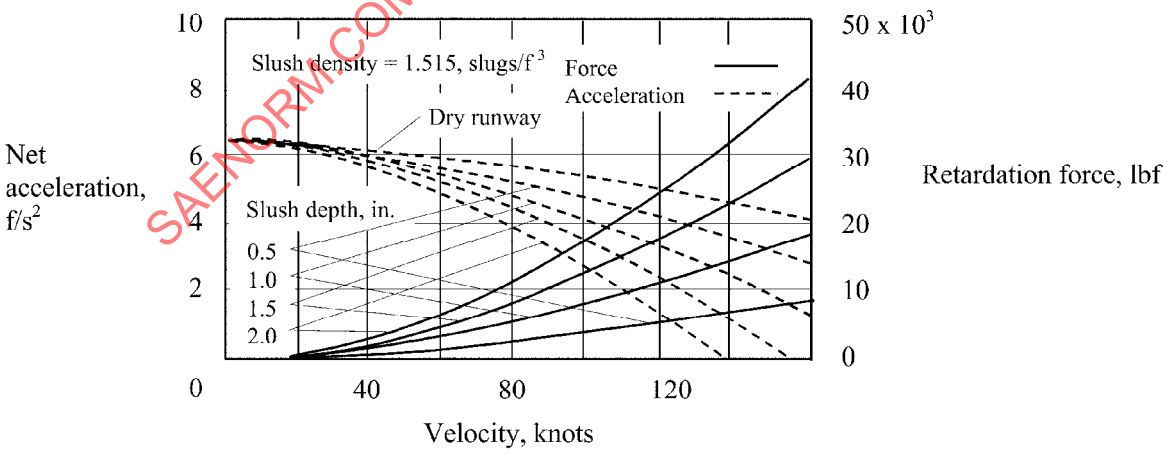

FIGURE 2 - Effect of Slush Depth on the Takeoff Distance Required for a Four-Engine Jet Transport Operating at 210,000 lbf Gross Weight With 13,000 Pound Thrust Engines (From NASA TN-D 552)

4.1 (Continued):

Generally, the slush drag effects on the tires increase parabolically up to the tire hydroplaning speed, and then drop off as the tire rides up on the water or slush during total hydroplaning. While it might seem that total slush drag on the aircraft would lessen at this point, such may not be the case. The amount of impingement drag on the airframe caused by the intense spray that is sent up from the hydroplaning tires may exceed the tire drag, and thus the acceleration of the aircraft could be reduced appreciably at this point. These factors may place a large responsibility on the design of tires and landing gear to be able to deflect water and slush clear of the airframe.

f. Erosion or structural damage to rear mounted (pusher) propellers.

4.2 Spray Geometry:

Current knowledge of water spray geometry is very limited. Research conducted at NASA Langley Research Center in the mid 1980's forms the bulk of this information. These tests were conducted at the Hydrodynamics Research Facility, an enclosed 2900-foot long water tank. The tests were conducted with a 6.00 X 6, TT, 8-ply rating, Type III aircraft tire typical of a nose gear tire for a 6000 pound class twin-engine, general aviation aircraft. A few tests were also conducted with 26 X 6.6 tubeless, 12-ply rating, Type VII aircraft tires of bias-ply and radial belted design. A 22-tube X 22-tube water collector array shown in Figure 3 was used to collect water from the tire water spray plum. Each tube was 1.625 in. inside diameter. Tests were conducted with the water collector array located 31-, 76-, and 199-inches behind the test tire. A schematic of the water collector array locations is shown in Figure 4. Results from these tests are reported in NASA Technical Paper 2718 and SAE Technical Paper 861626 and will be summarized here.

4.2.1 Bow Wave and Rooster Tail Trajectories: As an aircraft tire rolls through a body of standing water on a flooded runway, the water in the path of the tire must be displaced if the tire velocity is below the hydroplaning speed.

The majority of the water along the tire path is displaced laterally. However there is a small amount of water that exits the tire path in a "bow wave" ahead of the tire, and some additional water that is expelled from the rear of the tire in a "rooster tail" plume as shown in Figure 5. Extensive high-speed photography of the bow wave and rooster tail plumes from the NASA tests indicate that the amount of water in these plumes is relatively small and quickly atomized into small droplets. As a consequence, these two plumes may contribute very little water spray for ingestion into the engine. It should be noted, however, that the water in these plumes may cause damage to antennae or other sensitive systems if they are located in an impingement zone of the airframe.

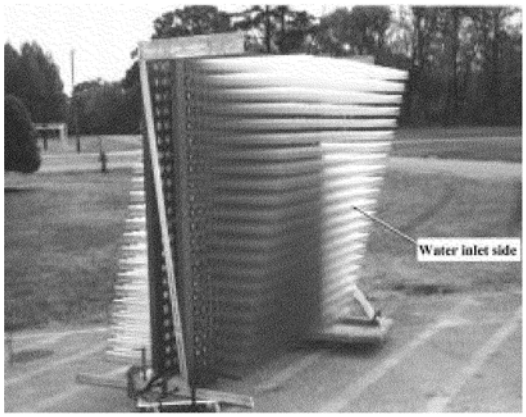

FIGURE 3 - Water Collector Array Used in NASA Tests

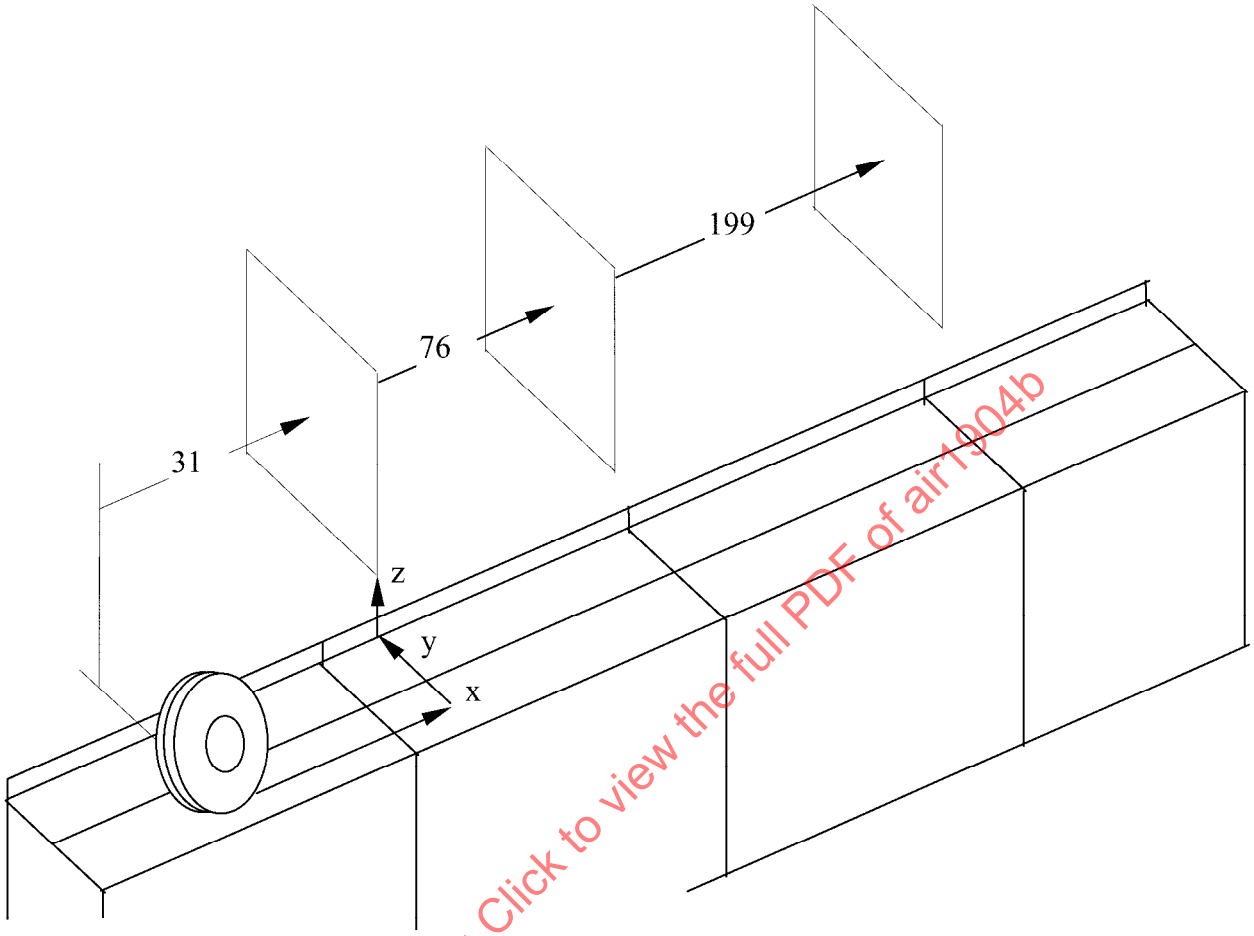

FIGURE 4 - Test Runway, Nose-Tire, and Water Spray Collector Measurement Positions
All Dimensions in Inches

- Side or firehose spray
  - Sprays out from side of tire
  - Dense, concentrated stream of water

- Bow wave
  - Sprays out from front of tire
  - Usually a fine mist
  - Spray angle diminishes as hydroplaning speed is approached
  - Bow wave disappears above hydroplaning speed
  - Most severe at or below ground speed of 60 knots

- Rooster tail, dual wheels
  - Caused by impingement of two side sprays on each other from closely spaced wheels
  - Dense stream of water

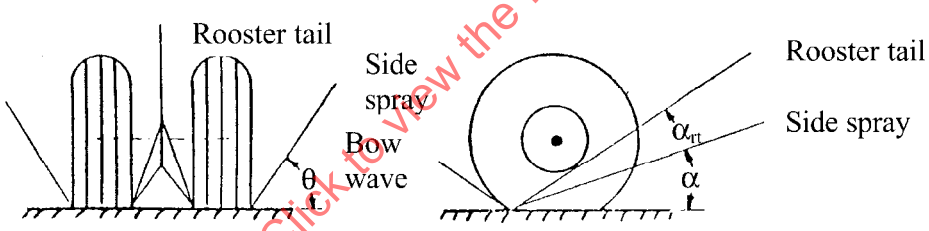

- Rooster tail, single wheel
  - Caused by adhesion of water to tire and thrown out of grooves by centrifugal force
  - Wide spray angle
  - Lighter consistency
  - Generally higher speed ranges
  - Characteristically splashes off airplane and may be redirected into engine

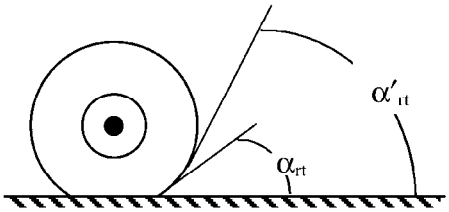

FIGURE 5 - Definition of Water Spray Types and Patterns

4.2.2 Side Plume and Wake Trajectories: The major contributor of water for ingestion into the engine is the laterally displaced water from the tire path. There are two sources of water associated with this lateral displacement. The first source is, of course, the side plums of water displaced directly from the tire footprint. As this water moves laterally, it interacts with the initially undisturbed water outside the tire path. This collision of laterally moving water with the adjacent water creates a wake or lateral wave to form in the initially undisturbed water. The NASA tests indicate that there is enough energy in this wake action to throw a considerable amount of additional water into the air. The volume of water associated with this wake action can be from 5 to 10 times the water volume directly in the path of the tire. A photograph and sketch depicting this wake induced water spray plume is shown in Figure 6.

Figure 7 shows an analytically derived schematic of the lateral water spray plume from a series of NASA tests conducted at an aircraft velocity of 40 f/s. The trajectory shown in the figure exhibits an initial azimuth plume angle of 43 degrees and an angle of 11 degrees forward in the ground plane. The initial speed of water leaving the footprint was about 66 f/s. Note that the trajectory of the lateral plume shown in Figure 7 has a forward velocity component that is greater than the aircraft velocity.

4.2.3 Effects of Various Test Parameters on Water Spray Plumes from NASA Tests: Figure 8 presents summary plots of curves depicting the most concentrated regions of the various water spray plumes for several different test conditions. At the base of each curve, the maximum normalized flow rate is shown in ($in^3/min/in^2$). The ending flow rate for each test condition is also shown at the top of each curve.

Figure 8(a) shows the variation in plume intensity as the water collector array is positioned at three different locations aft of the test tire. These tests were conducted at a speed of 60 f/s, a tire load of 2500 pounds force, a tire inflation pressure of 35 psi, and a water depth of 0.625 inches. The slopes of the three curves depicting the centroid of the water spray plume at various distances behind the test tire suggest that there is a fairly complicated interaction between the side plume associated with the water displaced from the tire footprint and the water thrown upwards from the tire wake.

The effect of speed on the water spray side plume is shown in Figure 8(b). These tests were conducted at a tire load of 2500 pounds force, a tire inflation pressure of 35 psi, and a water depth of 0.625 inches. The water collector array was 199 in. aft of the test tire. The data in the figure indicate that the intensity of the spray plume increases with increasing ground speed over the range of speeds tested. These data also indicate a tendency for the water spray plume to move inboard as the speed increases.

The effect of tire load on the intensity and trajectory of the water spray plume is shown in Figure 8(c). These tests were conducted at a speed of 60 f/s, a tire inflation pressure of 35 psi, and a water depth of 0.625 inches. The water collector array was 199 in. aft of the test tire. The data in this figure indicate that for the 6.00 x 6 tire, heavier tire loads tend to cause the spray plume to move inboard relative to the lighter tire loads over the range of loads tested. The lighter loaded tire tends to concentrate the most intense portion of the water spray plume closer to the ground, whereas the heavier tire loads tend to throw more water higher into the air.

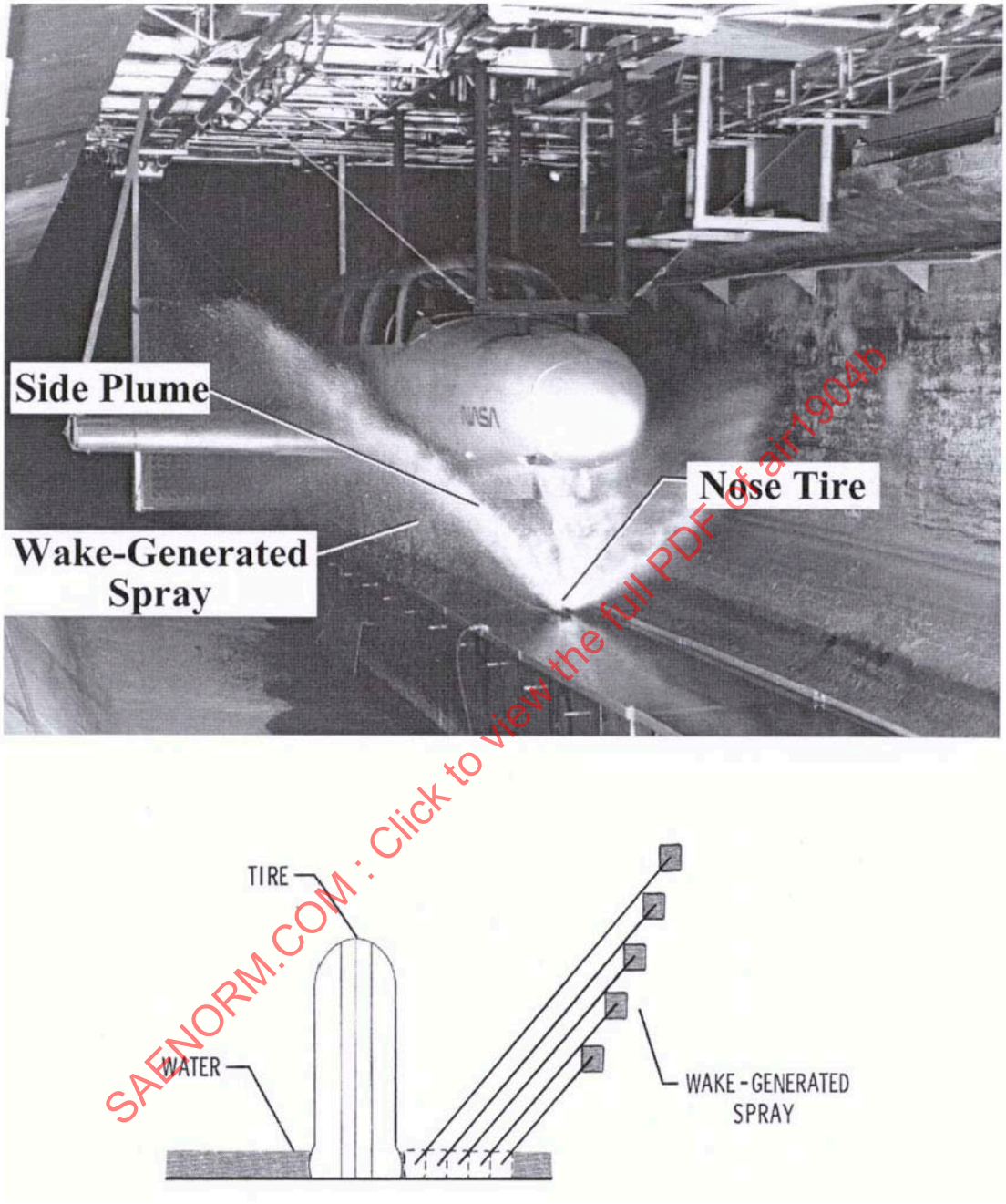

FIGURE 6 - Photograph and Sketch of Water Wake Phenomenon

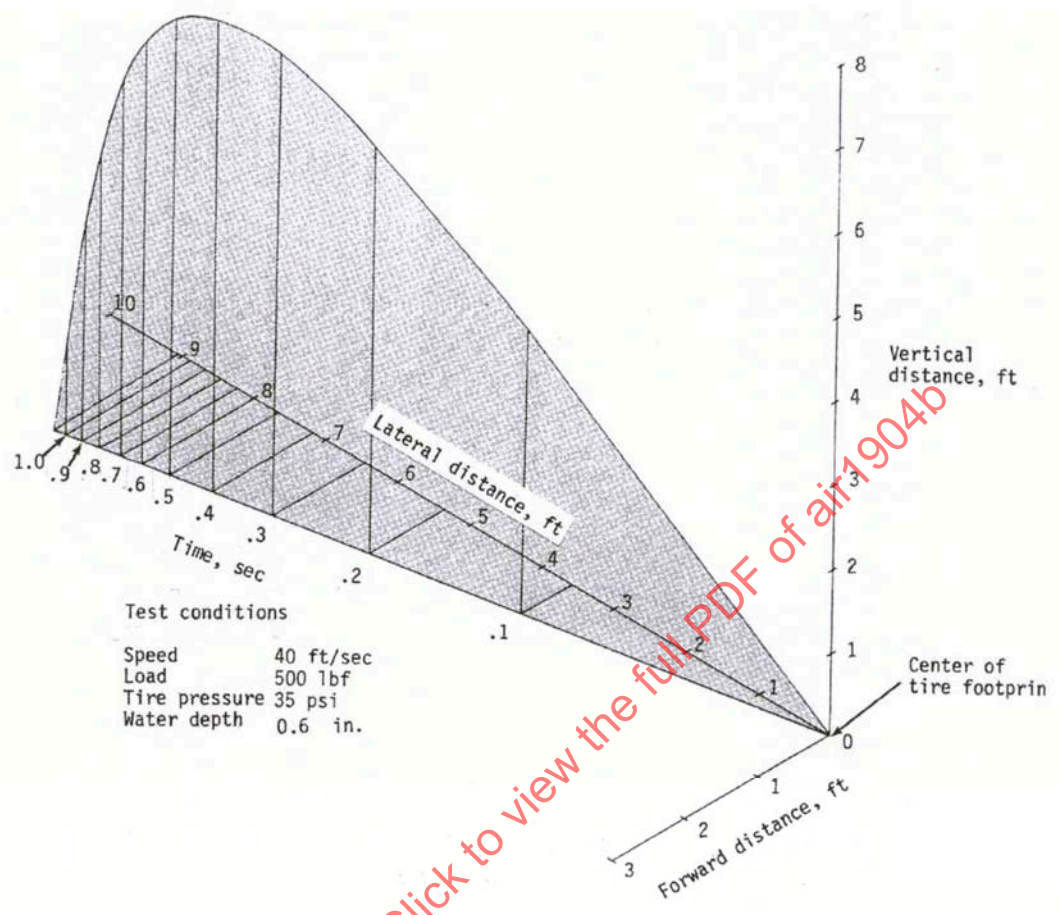

FIGURE 7 - Water-Spray Trajectory from Nose-Gear Tire

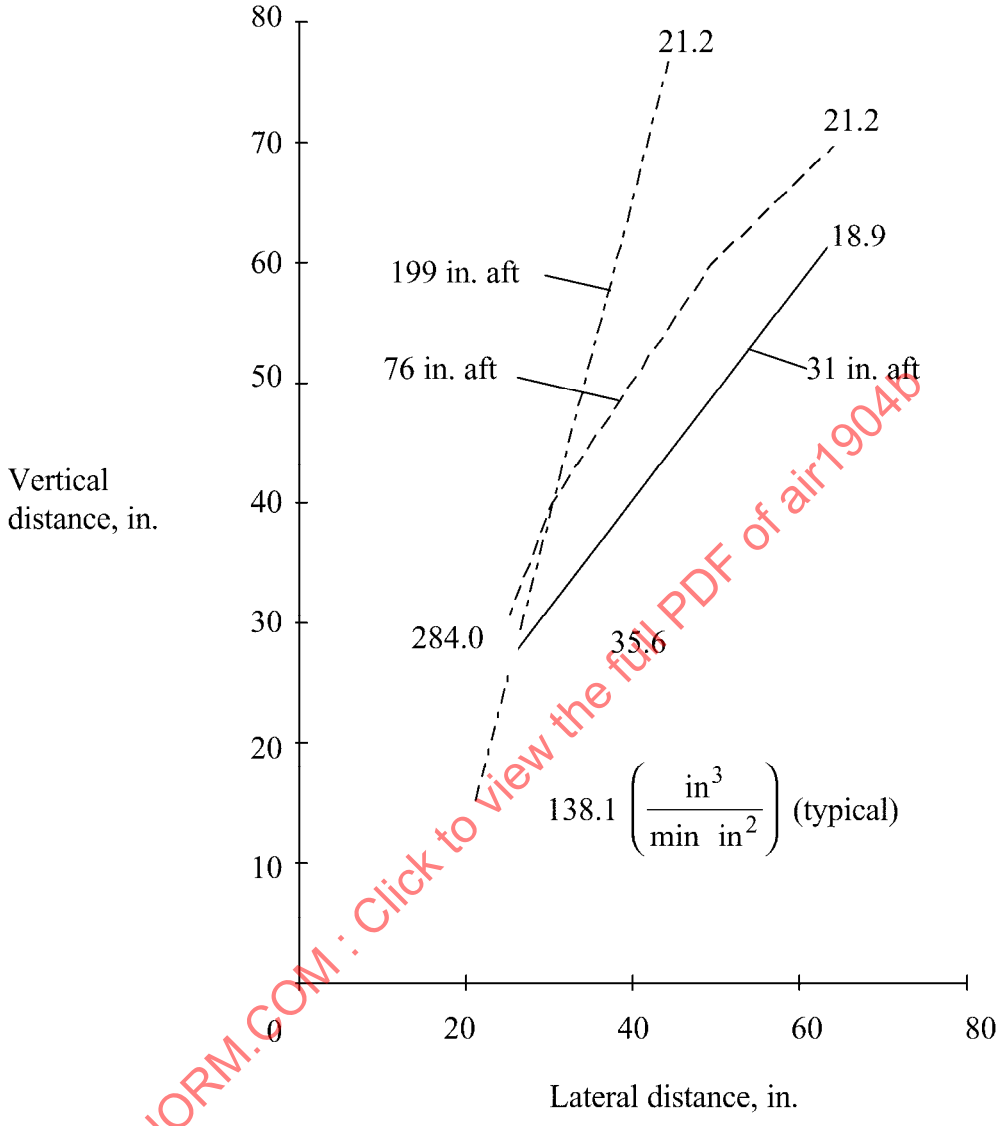

(a) Effect of distance aft. Speed, 60 f/s; tire load, 2500 lbf; inflation pressure, 35 psi; water depth, 0.625 in.

FIGURE 8 - Water-Spray Flow Concentration $\left(\frac{in^3}{min\ in^2}\right)$

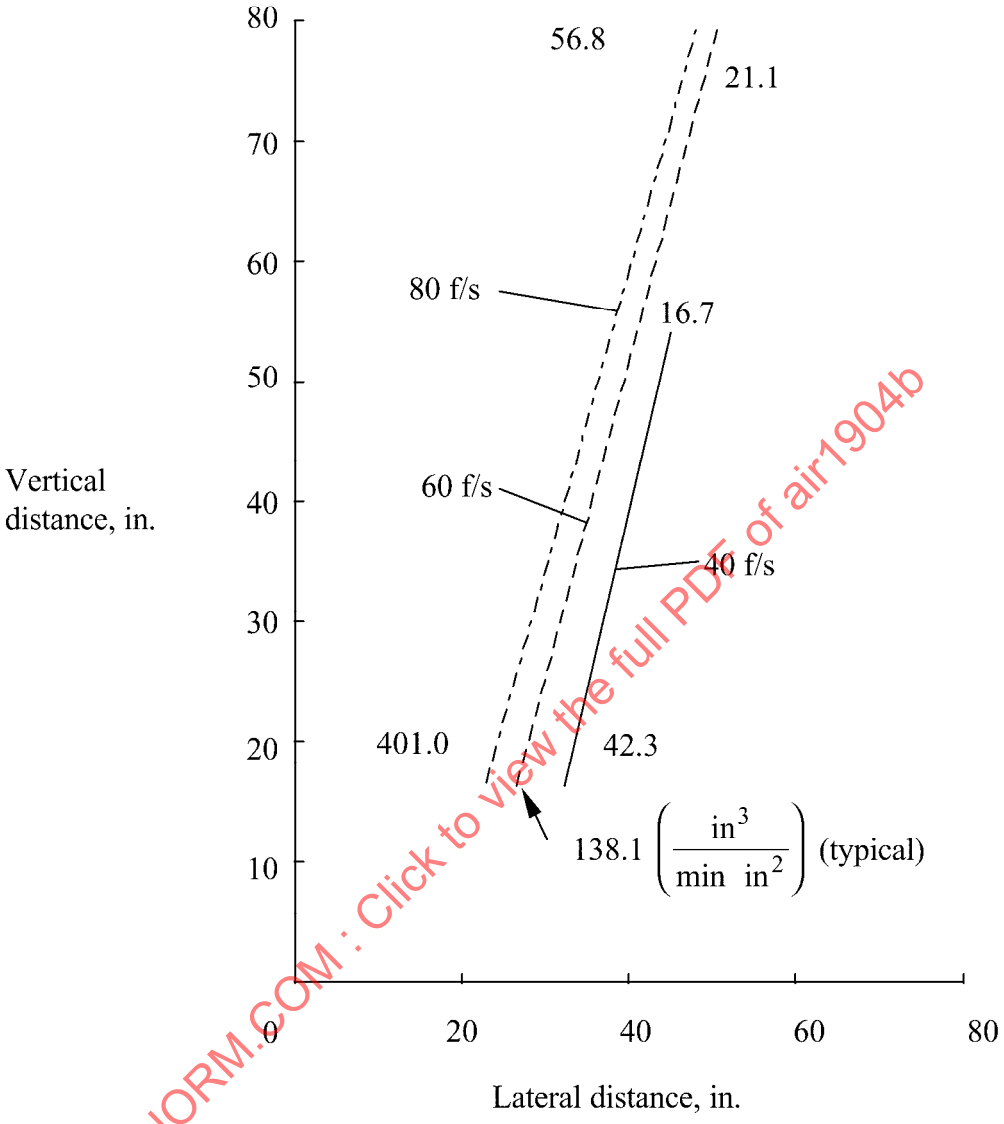

(6) Effect of speed. Tire load, 2500 lbf; inflation pressure, 35 psi; water depth, 0.625 in.; water-spray collector, 199 in. aft of tire.

FIGURE 8 - Water-Spray Flow Concentration $\left(\frac{in^3}{min\ in^2}\right)$ (Continued)

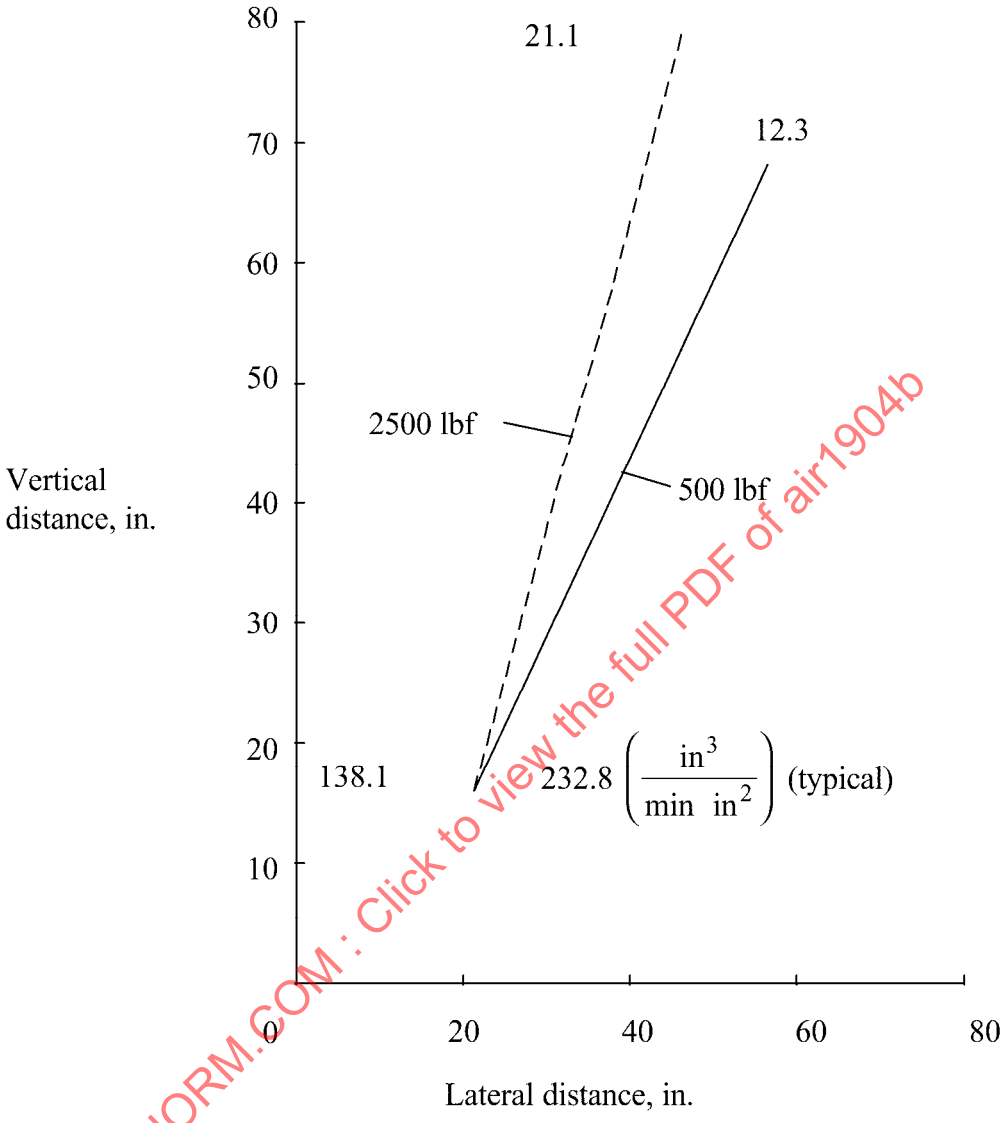

(c) Effect of tire load. Speed, 60 f/s; inflation pressure, 35 psi; water depth, 0.625 in.; water-spray collector, 199 in. aft of tire.

FIGURE 8 - Water-Spray Flow Concentration $\left(\frac{in^3}{min\ in^2}\right)$ (Continued)

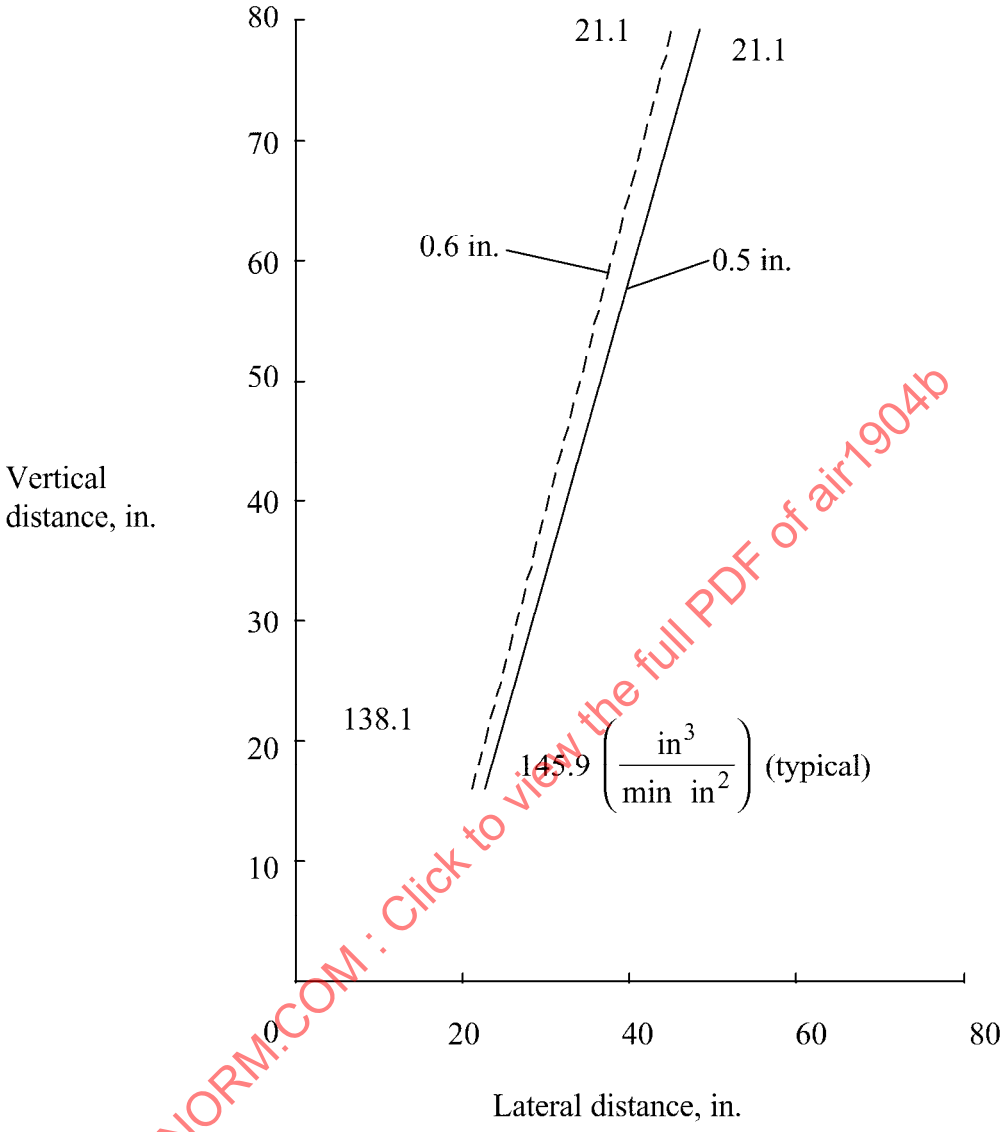

(d) Effect of water depth. Tire load, 2500 lbf; inflation pressure, 35 psi; speed, 60 f/s; water-spray collector, 199 in. aft of tire.

FIGURE 8 - Water-Spray Flow Concentration $\left(\frac{in^3}{min\ in^2}\right)$ (Continued)

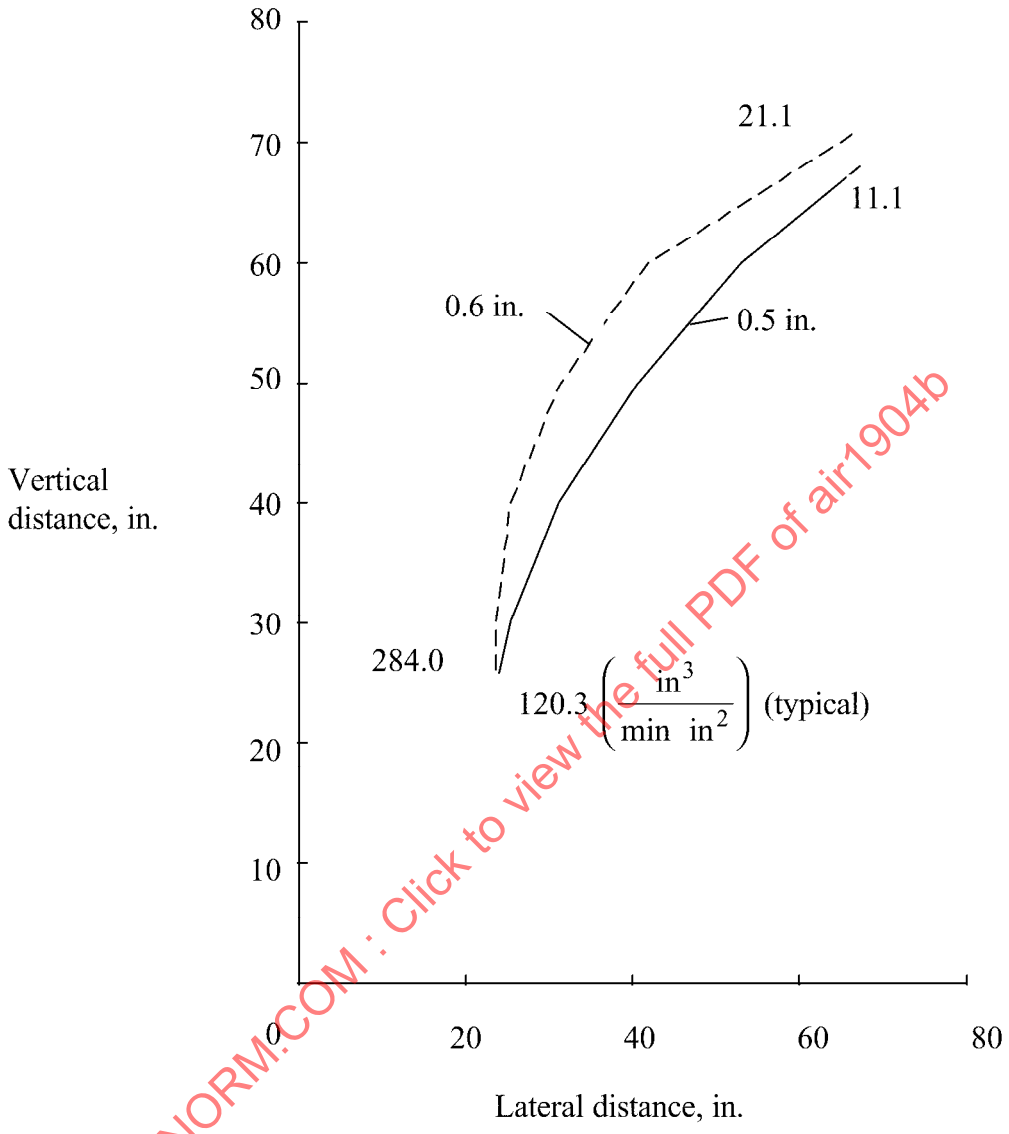

(e) Effect of water depth. Tire load, 2500 lbf; inflation pressure, 35 psi; speed, 60 f/s; water-spray collector, 76 in. aft of tire.

FIGURE 8 - Water-Spray Flow Concentration $\left(\frac{in^3}{min\ in^2}\right)$ (Continued)

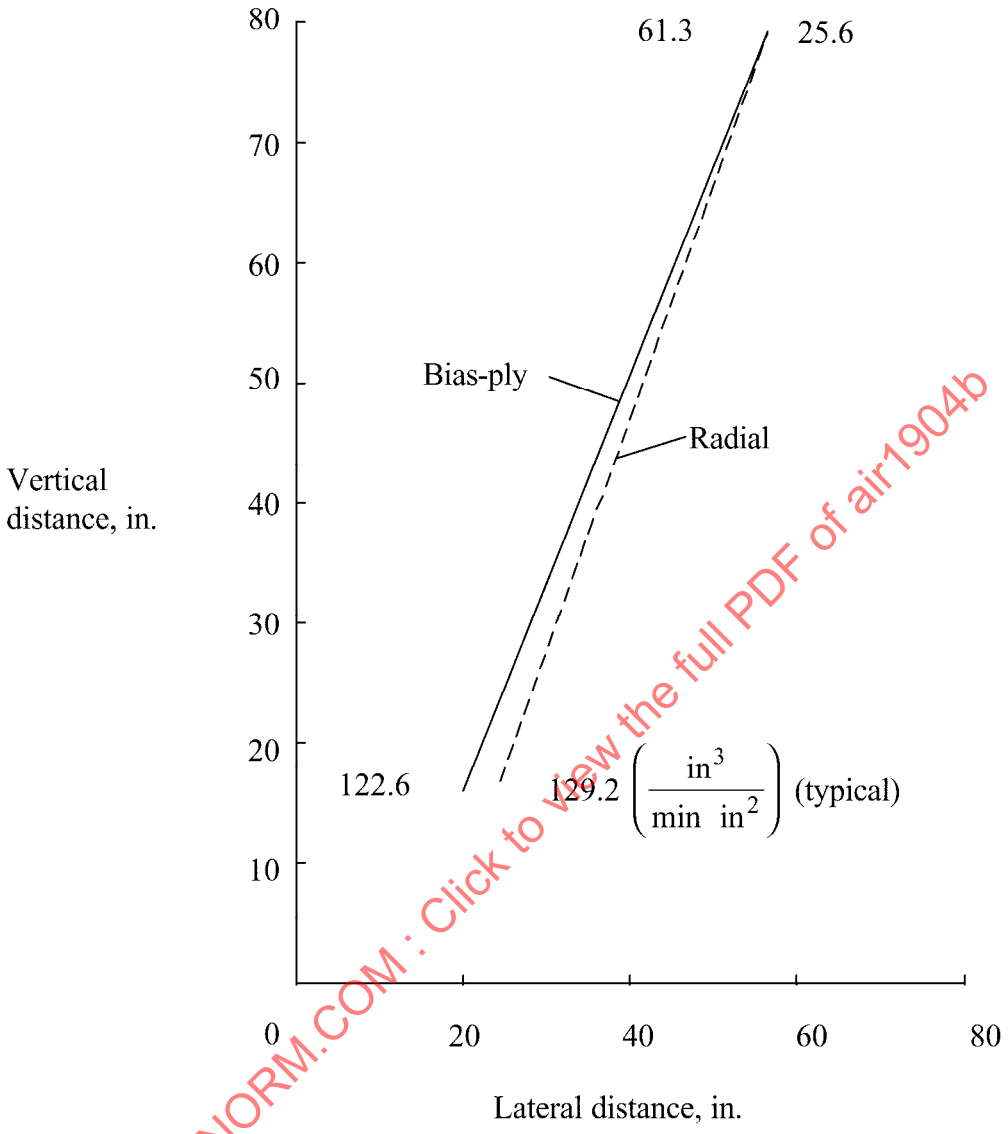

(f) Effect of tire construction, 26 x 6.6 aircraft tires. Inflation pressure, 45 psi; water depth, 0.625 in.; water-spray collector, 199 in. aft of tire; radial tire deflection, 1.9 in.; bias-ply tire deflection, 1.8 in.

FIGURE 8 - Water-Spray Flow Concentration $\left(\frac{in^3}{min\ in^2}\right)$ (Continued)

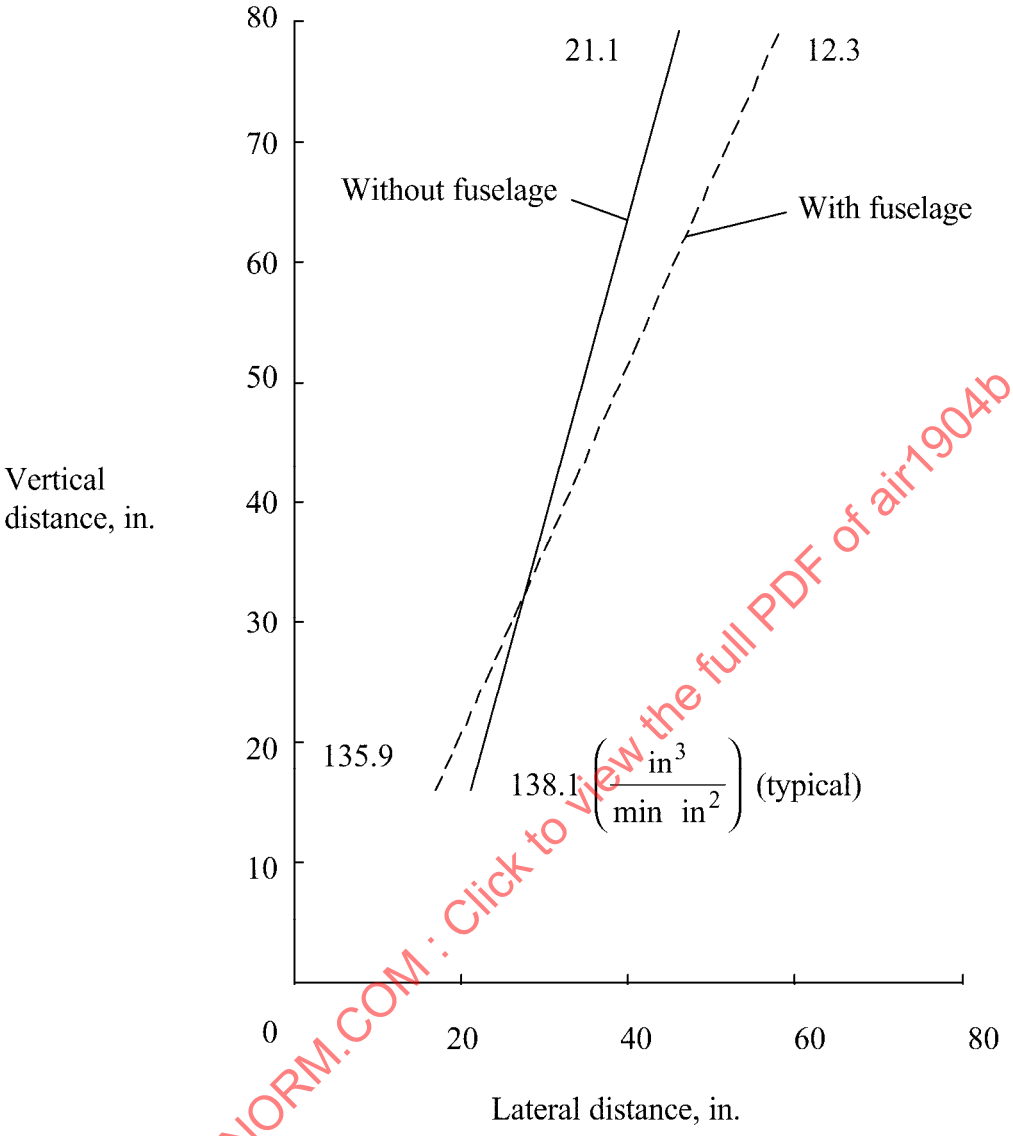

(g) Effect of fuselage. Tire load, 2500 lbf; inflation pressure, 35 psi; speed, 60 f/s; water depth, 0.625 in.; water-spray collector, 199 in. aft of tire.

FIGURE 8 - Water-Spray Flow Concentration $\left(\frac{in^3}{min\ in^2}\right)$ (Concluded)

4.2.3 (Continued):

The effect of water depth on the intensity and trajectory of the water spray plume is shown in Figures 8(d) and 8(e). These tests were conducted at a speed of 60 f/s, a tire load of 2500 pounds force, a tire inflation pressure of 35 psi, and at water depths of 0.5 and 0.6 inches. The water collector array was 199 in. aft of the test tire in Figure 8(d) and 76 inches aft of the test tire in Figure 8(e). The plumes for the two water depths tested were essentially the same at a position of 199 inches aft of the test tire. At a position of 76 inches aft of the test tire, the shape of the two trajectories were similar but the intensity of the water flow for the plume generated at a water depth of 0.6 inches was about twice as high as the plume intensity observed at a water depth of 0.5 inches.

The effect of tire construction on the water spray plume is shown in Figure 8(f). For these tests 26 x 6.6 bias-ply and radial-belted tires were used. The speed was 60 f/s, tire inflation pressure was 45 psi, tire loads were adjusted to give the bias ply tire a vertical deflection of 1.8 inch and the radial-belted tire a vertical deflection of 1.9 inch, and the water depth was 0.625 inch. The water collector array was 199 in. aft of the test tire. For the test conditions shown, the trajectory and intensity of the spray plumes for the two tires were similar.

Fuselage effects were simulated by conducting tests with a fuselage present and without a fuselage in Figure 8(g). These tests were conducted at a speed of 60 f/s, a tire load of 2500 pounds force, a tire inflation pressure of 35 psi, and a water depth of 0.625 inches. The water collector array was 199 in. aft of the test tire. The presence of the fuselage tends to move the trajectory of the water spray plume slightly outboard the trajectory generated without the presence of a fuselage. The intensity of the two plumes is about the same, however.

A series of tests were also run to determine the effect of the presence of both a fuselage and a wing on the water spray plume. Figure 9 is a schematic of the fuselage and wing geometry used in these tests. Two different wing positions were used. In the wing forward position, the wing root was 45 inches behind the test tire. In the wing aft position, the wing root was 99 inches behind the test tire. These series of tests were conducted at a tire load of 2500 pounds force, a tire inflation pressure of 35 psi, and a water depth of 0.625 inches. The water collector array was 199 in. aft of the test tire. The wing forward test condition caused the majority of the water spray plume to be deflected under the wing. The wing aft test condition resulted in an altered spray trajectory in which a portion of the water spray was deflected upward, apparently due to wing aerodynamic effects.

Figure 10 summarizes the NASA water spray flow rate data originally presented in Figure 8. The data in Figure 10 are from an internal Boeing (formerly McDonnell Douglas) document. In Figure 10 the non-dimensional flow rates for tests that did not involve the general aviation wing and fuselage are plotted as a function of non-dimensional velocity squared. These results indicate that the intensity of the side-spray flow rates increases with velocity over the range of test conditions examined during the NASA tests.

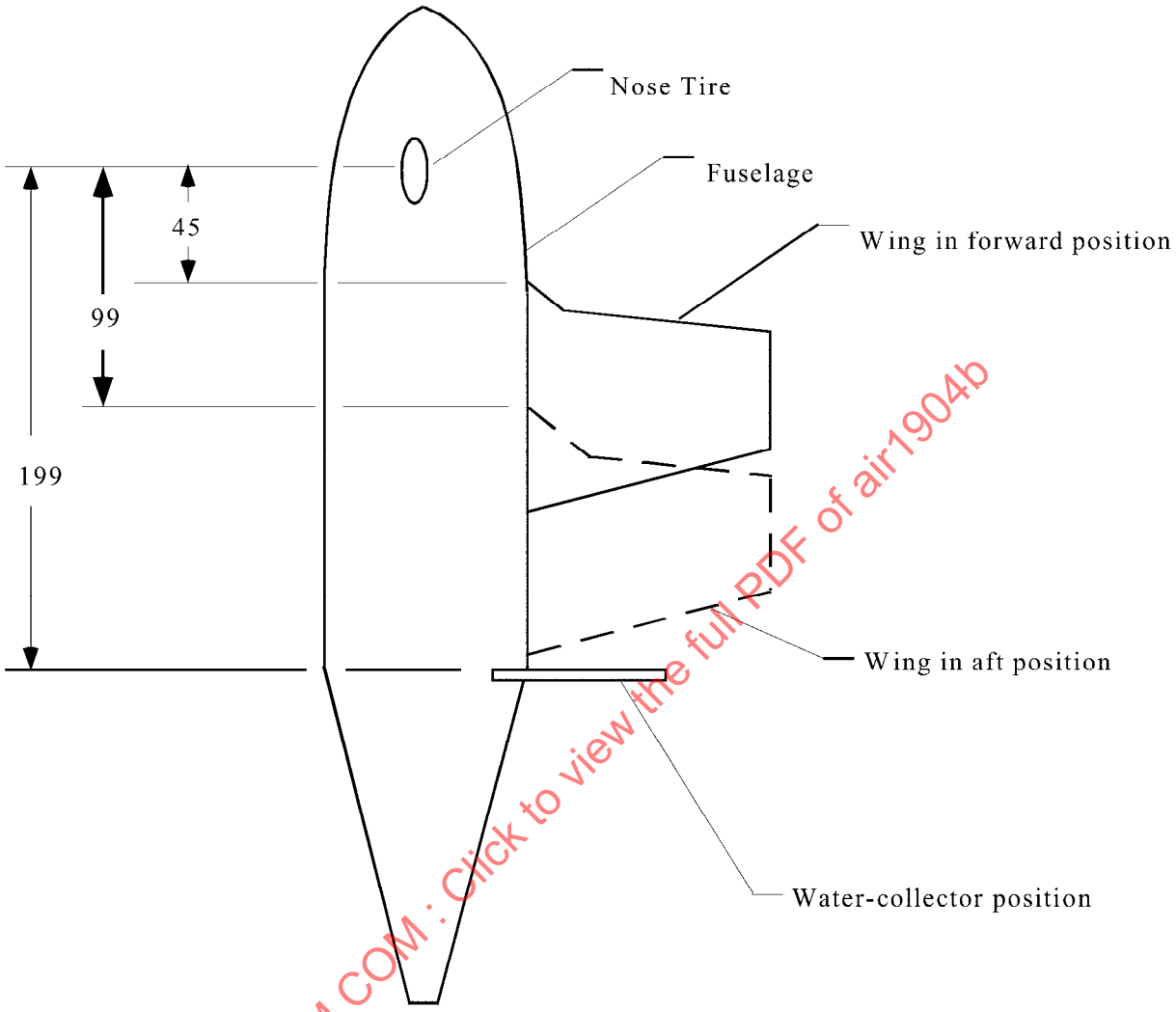

NOTE: This configuration is applicable to a specific test. Modifications should be anticipated for each airframe and tire combination.

FIGURE 9 - Schematic of Fuselage, Wing, and Water Collector

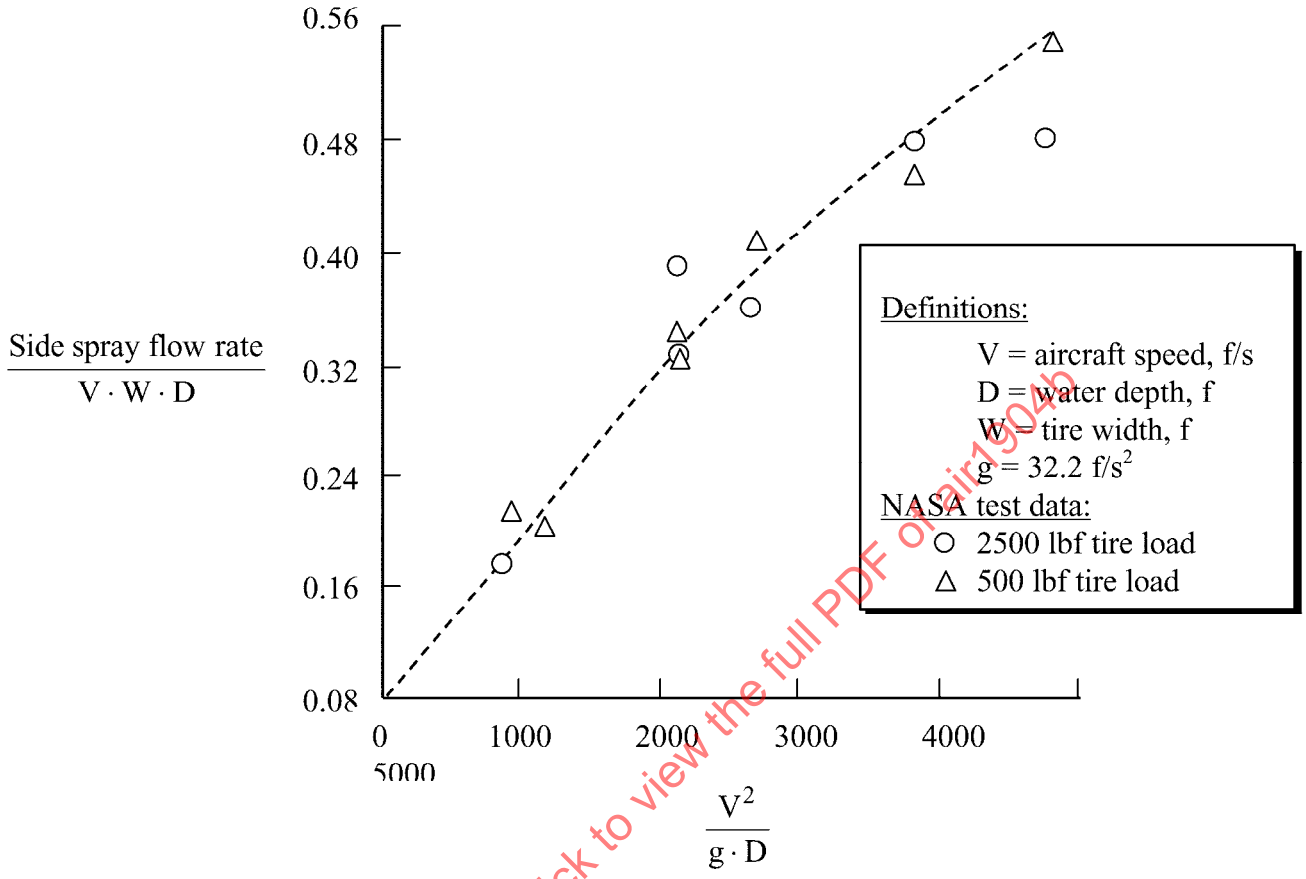

FIGURE 10 - Relationship Between Spray Flow Rate, Aircraft Speed, and Water Depth for NASA Tests

4.2.4 Flight Testing Conducted at the Royal Aircraft Establishment of England (RAE) and the Boeing Company (formerly the McDonnell Douglas Corporation): Over the years aircraft manufacturers and research organizations have conducted aircraft flight tests on flooded runways to establish the water spray characteristics for specific airplane applications. Figures 11 and 12 summarize limited flight test data from the Royal Aircraft Establishment of England (RAE) and the Boeing Company (formerly the McDonnell Douglas Corporation) and present comparisons of water spray plume angles from these tests with the NASA data. Table 1 provides additional data on the range of test parameters for the three data sets.

TABLE 1 - Spray Ingestion Test Parameter Ranges

	Tire pressure, (psi)	Water depth, (in.)	Velocity, (f/s)
NASA	35-45	0.6-0.625	40-80
RAE	68-106	0.58-2.0	68-186
McDonnell Douglas	105-170	0.5-1.0	196-208

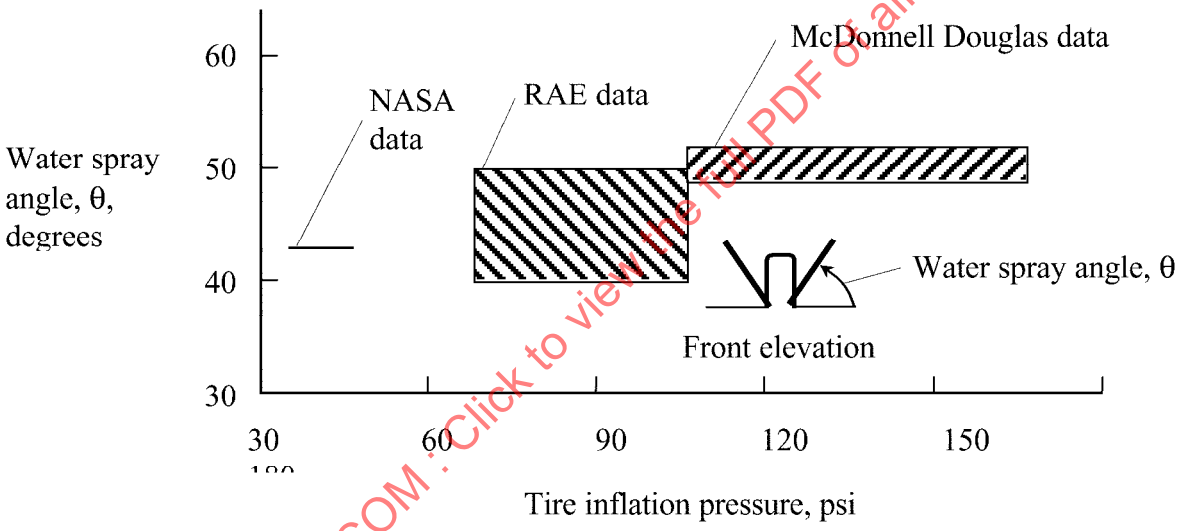

FIGURE 11 - Comparison of Side Spray Angles, θ, Obtained From Three Different Sources

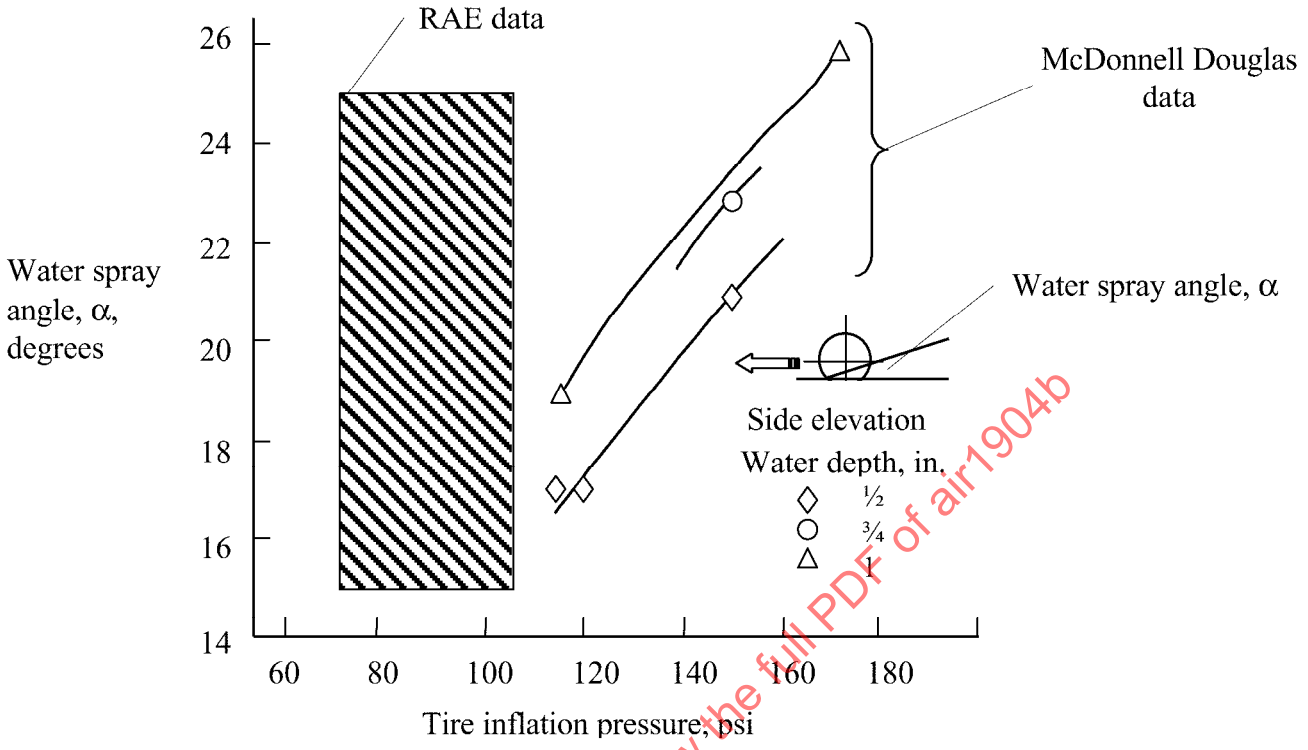

FIGURE 12 - Comparison of Side Spray Angles, α, Obtained From Two Different Sources

4.2.4 (Continued):

During the 1960's the RAE conducted flooded runway flight tests with three different airplanes: a Canberra, an Ambassador, and a Viscount. These tests were conducted on the RAE runway in Bedford, England. McDonnell Douglas conducted flooded runway flight tests with both the DC-9 and DC-10 aircraft. These tests were run at the NASA Wallops Island Flight Test Facility in Virginia and in Roswell, New Mexico respectively. In Figure 11 lateral water spray angle θ data from NASA, RAE, and McDonnell Douglas are plotted as a function of tire inflation pressure. Comparisons of the data from the three sources suggest a tendency for the lateral water spray angle to increase slightly with increasing tire inflation pressure. It should be noted, however, that the perceived tire pressure effect in Figure 11 could also be the result of velocity and/or water depth differences among the three data sets depicted in Table 1. The range of lateral water spray angles θ for all the tests shown in Figure 11 is from 40 degrees to about 52 degrees.

In Figure 12 water spray angle α data from the RAE and McDonnell Douglas are plotted as a function of inflation pressure. The range of water spray angles for the two sets of data range from about 15 degrees to approximately 26 degrees.

4.2.5 Analytical Models of Water Spray Trajectories: Landing gear specialists at Boeing (formerly the McDonnell Douglas Corporation) developed a system of differential equations and initial conditions to predict the water spray trajectories developed by aircraft tires on flooded runways. These equations and initial conditions and comparisons between the measured and predicted trajectories are presented in the following paragraphs.

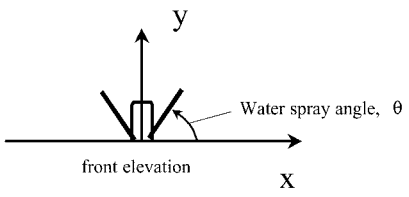

FIGURE 13

The governing differential equations and initial conditions in ground coordinates (x, y) are:

$$\frac{dy}{dt} = v \qquad \frac{dx}{dt} = u$$
$$\frac{dv}{dt} = -g - BC \cdot \frac{\rho u^2}{2} \qquad \frac{du}{dt} = -BC \cdot \frac{\rho u^2}{2} \qquad \text{(Eq. 1)}$$

At t = 0:

$$x = x_j \qquad u = V_w \cos\theta_w$$
$$y = y_j \qquad v = V_w \sin\theta_w \qquad \text{(Eq. 2)}$$

Where:

u: water spray velocity in x direction, f/s
v: water spray velocity in y direction, f/s
ρ: density of air, slugs/f^3
g: gravitational acceleration, f/s^2
BC: lumped ballistic coefficient, equal to $\left(\frac{C_D \cdot A}{m}\right)$
C_D: drag coefficient
A: projected area of water spray, f^2
m: mass of water, slugs
x_j and y_j: initial coordinates of water spray at tire-ground interface, f

4.2.5 (Continued):

V_w: initial velocity of water spray, f/s
θ_w: initial water spray angle (front elevation), degree

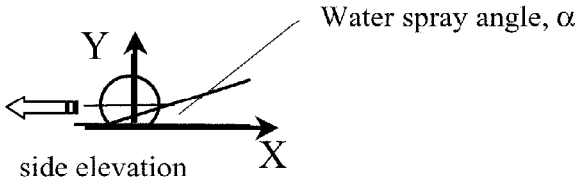

FIGURE 14

$$Y(t) = Y(t) + y_j$$
$$X(t) = U \cdot t + x_j$$

Where:

U: aircraft velocity, f/s

A comparison of a measured and predicted water spray trajectory from the NASA tests is presented in Figure 15. In the figure the water spray trajectory height is plotted as a function of the outboard displacement of the water spray plume from the nose-gear tire. For the NASA test the initial velocity of the water spray was taken as 66 f/s, the initial water spray angle was assumed to be 43 degrees above the horizontal plane, and the ballistic coefficient was assigned a value of 203. The analytical prediction and measured water spray trajectories, as viewed from a front elevation are in good agreement up to the point of maximum water spray height. The maximum outboard displacement of the spray plume was about 10 feet as measured during the NASA test and the analytical model predicts a maximum outboard displacement of about 11 feet.

A comparison of the measured and predicted water spray trajectory from a McDonnell Douglas flight test is presented in Figure 16. In this figure the water spray trajectory height is plotted as a function of distance aft the nose-gear tires. For these flight test conditions the initial water spray angle was taken as 43 degrees and the ballistic coefficient was assumed to be 130. The initial water spray velocity was approximated by the ratio of initial aircraft velocity to velocity of the NASA test and was set to 320 f/s for these test conditions. The analytical prediction and measured water spray trajectories, as viewed from a side elevation in Figure 16, are in good agreement up to the point of maximum water spray height (about 14 feet for this test condition).

The fact that the ballistic coefficient was assigned two different values in Figures 15 and 16 to approximate experimental data suggests that additional research is needed to establish the effect of test parameters such as tire pressure, aircraft velocity and water depth on the ballistic characteristics of water spray plumes.

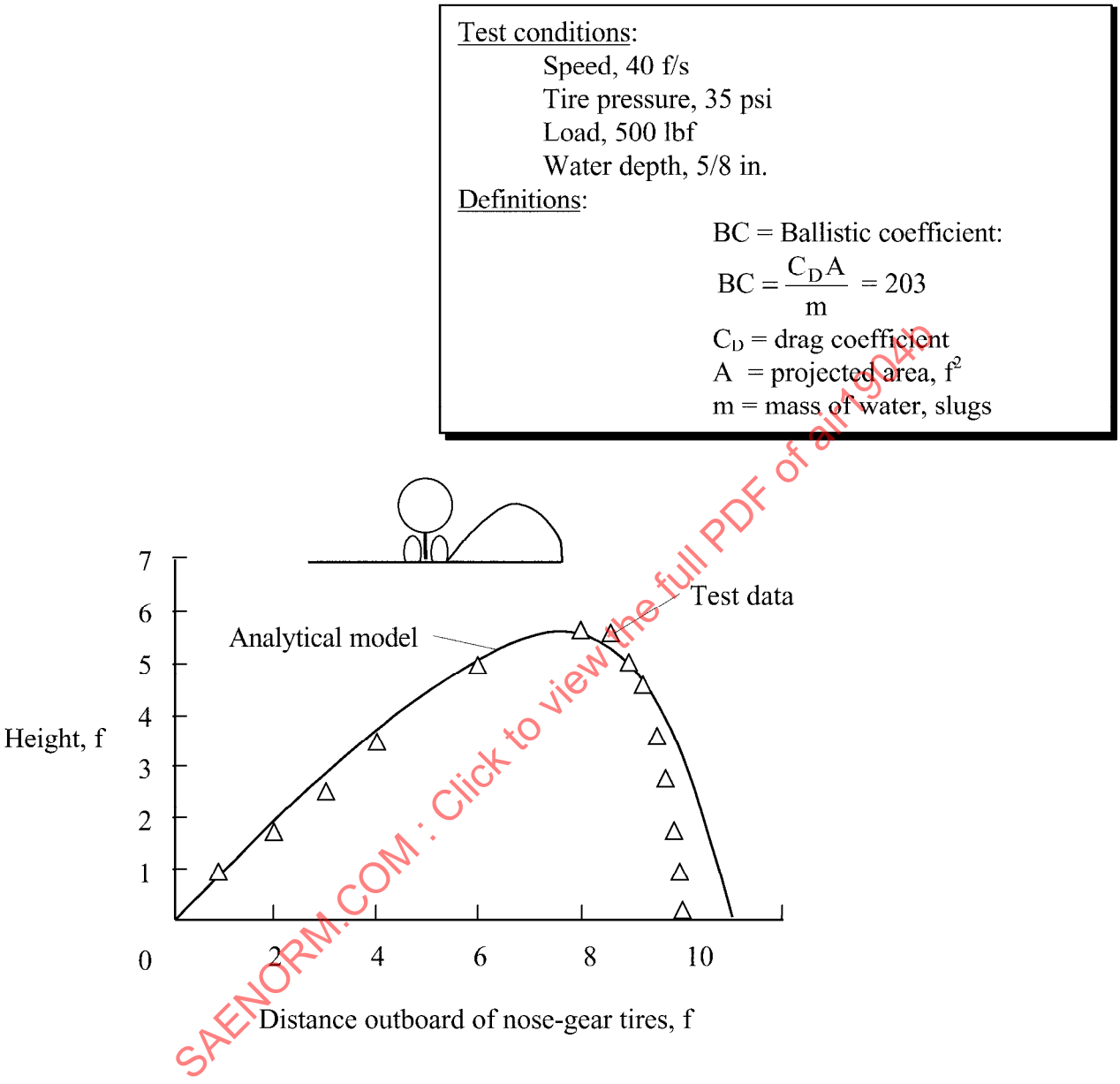

FIGURE 15 - Comparison of Water Spray Trajectory Prediction and Experimental Measurements from NASA Tests
V_w = 66 f/s; θ_w = 43 degrees

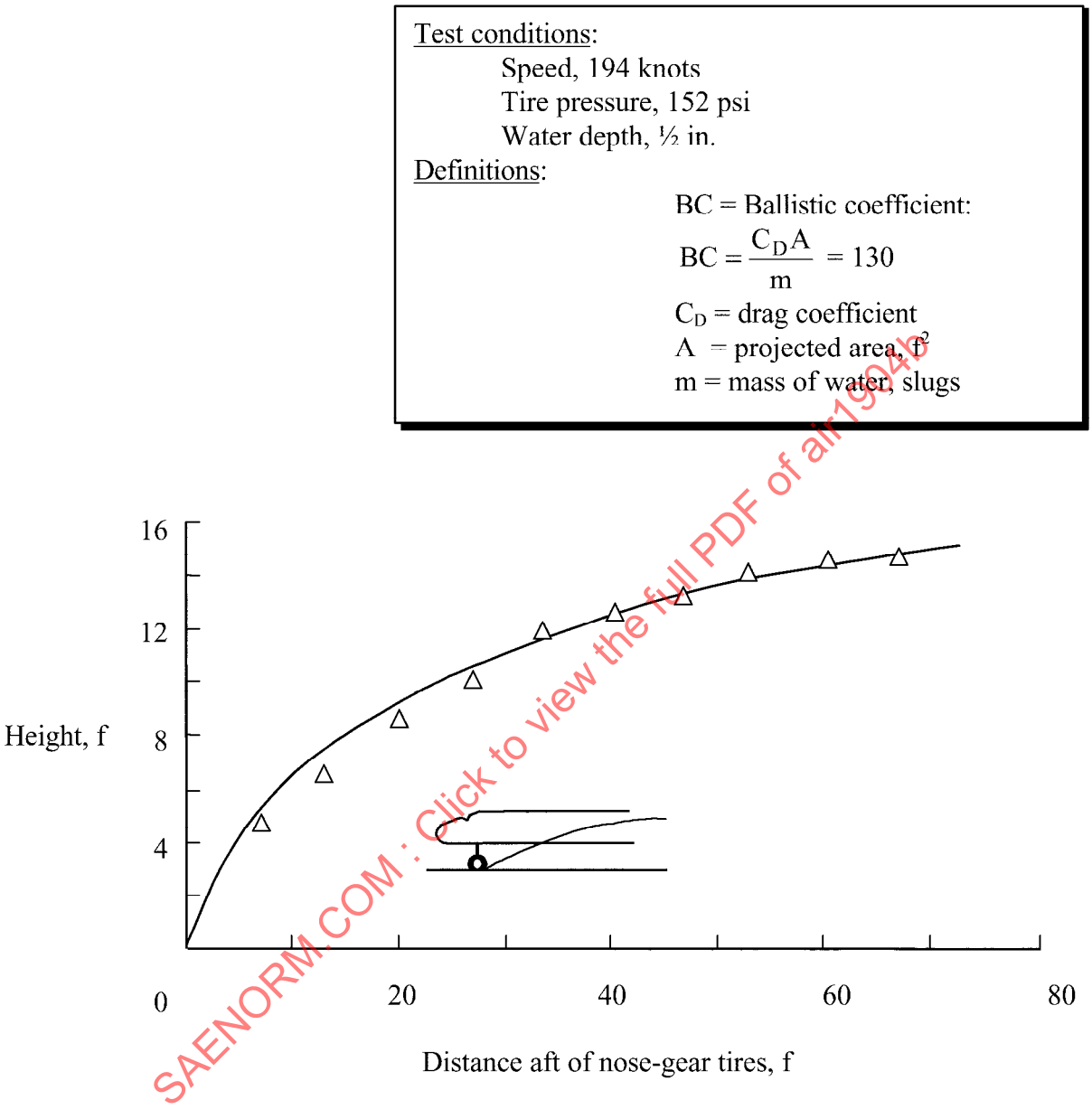

FIGURE 16 - Comparison of Water Spray Trajectory Prediction and Experimental Measurements from DC 10-10 Flight Tests
V_w = 320 f/s; θ_w = 43 degrees

4.2.6 Consideration for Engine Capabilities (compare to engine manufacturer's limits):

1. Tire bow wave spray.
2. Tire side plume.
3. Tire "rooster tail" plumes.
4. Slugs of water or slush. (Concentrated verses evenly dispersed ingested materials. Engines are not certified for concentrated ingestion.)

NOTE: Spray geometry is affected by hydroplaning and should be examined at all certified ground operating speeds.

4.3 Airplane Parameters to Consider in Design:

a. Airplane velocity effect on tire shape (centrifugal forces on tire)
b. Tire pressure
c. Tire wear and tire tread profile design
d. Tire position in relation to other aircraft components, engines, wings, empennage, fuselage, etc.
e. Location of critical ports and mechanisms relative to spray patterns
f. Flight deck visibility effects
g. Aircraft loading variations

4.4 Water/Slush Depth to be Certified for Safe Operation:

a. May be greater for some missions than others - requires a variety of devices to cope with all.

b. Based on AC91-6, FAR 23.1091, and FAR 25.1091, FAA will certify water depth for which testing has been shown to be safe for all operating conditions.

c. Also of interest may be Advisory Circular No. AC 20-124 Water Ingestion Testing for Turbine Powered Airplanes.

4.5 Placement of Spray Suppression Devices:

a. Depends on source, type and severity of spray problems

b. Must maintain reasonably constant relationship to tire/runway interface

c. Must accommodate strut deflections and changing aircraft geometry relationships; such as, wing flaps, spoilers and thrust reversers

d. Must consider aerodynamic effect and stowage space if stowed

1. Consider possible powerplant-inlet airflow distribution

2. Assure space in wheel wells for safe gear operation - or other airframe or equipment clearances

4.6 Considerations for Water Spray Suppression Devices:

a. Chine tires:

1. Shape and placement, compatibility with tire technology

2. Effects of centrifugal forces (may change shape of chine)

3. Chine to runway clearance variations due to loading changes (tire deflection affects effectiveness)

4. Compatibility with normally expected variations in tire rolling radius due to variations in tire pressure, loads, tread wear, growth and manufacturing tolerances

5. Tire profile definition by airplane manufacturer so that multiple procurement sources may be approved on the basis of similarity (may control recapping also)

6. Compatibility with recapping procedures

7. Compatibility with maintenance methods

8. Compatibility with tow bars, spotting dollies, and other ground support equipment

9. Specifications for tires may be prepared to control variables and eliminate the need for qualification water testing due to different vendors and/or minor product changes. There is precedent for this procedure.

10. Both single and dual chines may be considered - single chines normally accompany dual wheel assemblies.

11. Some aircraft may be towed with nose gear torque links disconnected allowing greater than normal turning angles. Chine/deflectors should clear obstructions in such cases.

b. Deflector:

1. Proper shape, size, placement and strength

2. Capability of being retracted (if applicable)

3. Compatibility with normally expected variations in tire rolling radius due to variations in tire pressure, loads, tread wear, growth, manufacturing tolerances, flat tire (interference with deflector)

4. Reasonable accessibility for jacking, tire changes, etc.

4.6 (Continued):

5. Minimum drag
6. Compatible with icing conditions
7. Ease of installation and maintenance

4.7 Consider Operational Compatibility for Either Chine or Deflectors:

a. Any cornering constraints?

b. Effect of runway contact; such as, chine damage effect on tire balance

c. Damage sources

1. Airport equipment overruns
2. Foreign objects
3. Pavement drop-offs and steep ramps
4. Carrier deck hardware; cables, deck grooves, plate heads, etc.

d. Positive assurance of inability of a damaged device to jam gear in wheels-up configuration.

e. Consider effect of both grooved and ungrooved runways (if satisfactory on ungrooved runway probably okay on grooved runways). Tests are normally run on ungrooved surfaces.

f. Loss of steering effectiveness due to hydrodynamic lift (if used on steerable gear).

g. Compatible with uplocks, downlocks, and sensitive items around the landing gear.

4.8 Slush Versus Water Deflection:

Testing in specially prepared facilities where ice has been shaved into a test trough to create a thick, slurry or slush has been done, The Civil Aviation Authority (British) and Canadian Department of Transport have experience in this area with research and/or certification requirements placed on airframe manufacturers.

Reference to NASA Technical Note D-552 may be useful in regard to slush effects. That study focused on drag and indicates that water and slush have similar effects. Comments from airframe manufacturers indicate that water and slush are dynamically similar and that testing in water will adequately demonstrate performance for an equal depth of slush. It is evident that test conditions in water are more controllable due to the temperature effects on slush and the provisions to shave ice and manufacture slush.